

A major purpose of the Technical Information Center is to provide the broadest dissemination possible of information contained in DOE's Research and Development Reports to business, industry, the academic community, and federal, state and local governments.

Although a small portion of this report is not reproducible, it is being made available to expedite the availability of information on the research discussed herein.

LA-UR--88-4149

DE99 005462

Los Alamos National Laboratory is operated by the University of California for the United States Department of Energy under contract W-7405-ENG-36

TITLE: FREE ELECTRON LASERS USING STABLE-UNSTABLE RING RESONATORS

AUTHORS: Mark J. Schmitt, Mission Research Corporation
Alan H. Paxton, Mission Research Corporation

SUBMITTED TO **SPIE's Meeting of Optics**
 Electro-Optics and Laser Applications in Science
 and Engineering

Los Angeles, Airport Hilton, 15-20 January 1989

MASTER

By acceptance of this article, the publisher recognizes that the U.S. Government retains a non-exclusive, royalty-free license to publish or reproduce the published form of this contribution, or to allow others to do so, for U.S. Government purposes.

The Los Alamos National Laboratory requests that the publisher identify this article as work performed under the auspices of the U.S. Department of Energy.



Los Alamos

Los Alamos National Laboratory
Los Alamos, New Mexico 87545

Free Electron Lasers using Stable-Unstable Ring Resonators

Mark J. Schmitt and Alan H. Paxton

Mission Research Corporation, 127 Eastgate Drive, Suite 208
Los Alamos, New Mexico 87544

ABSTRACT

The free electron laser (FEL) simulation code FELEX is used to examine the operation of stable-unstable FEL resonators. These resonators are stable along one transverse axis and unstable along the orthogonal transverse axis. The simulations utilize a ring resonator with an intracavity focus in the unstable plane near the center of the wiggler (close to the same axial position as the waist in the stable plane) thereby enhancing the coupling between the optical and electron beams. Asymmetric output scraping is performed in the back leg of the ring using a reflective mirror inserted from one side of the unstable axis. Resonators with relatively low equivalent Fresnel number ($|N_{eq}| \leq 10$) and magnification ($|M_z| \approx 1.2$) are examined. Optical characteristics including the cavity mode profile at various positions inside the resonator are shown.

1. INTRODUCTION

The construction of laser oscillators with very high circulating powers requires the use of totally reflective optical elements. Such elements minimize the absorption of optical power and allow for mirror substrate cooling across the entire mirror aperture. Stable resonators employing these optical elements can only be out-coupled using either diffractive elements¹, halo scrapers or hole couplers. Unfortunately, each of these techniques suffers from at least one drawback. Diffraction gratings of significant size are difficult to fabricate and have significant losses; halo scrapers produce annular output beams that have inferior focus intensities and hole couplers produce a loss of on-axis intracavity intensity that reduces laser efficiency. One can avoid the use of these techniques by allowing the cavity geometry along one transverse axis to become unstable, such that an output coupling scheme previously described^{2,3} can be employed. This scheme involves asymmetrically scraping one edge of the circulating optical beam as shown in Figure 1. The position of the scraper edge dictates the size of the optical mode along the unstable axis. Since the cavity has a focus in the unstable plane, output scraping of only one side of the optical beam is required to limit the mode size at both edges. This is a consequence of the field inversion that occurs at the focus. Thus, each edge of the mode is scraped on every other pass through the cavity. This output coupling scheme also has the advantage that a filled-in output beam is produced which propagates to a central peak in the far field.

A study has been undertaken to examine the properties of this type of resonator for free electron laser applications. The three-dimensional code FELEX⁴ is being used to model both the optical propagation in the resonator and the interaction of the optical mode with the electron beam inside the wiggler. In Section 2 initial simulations are compared to previously published unstable cavity mode profiles for code validation purposes. These simulations include linear and ring geometries with and without intracavity foci. Simulation of the cavity of a stable-unstable dye laser currently in operation is conducted in Section 3. Subsequent simulations of the stable-unstable resonator with a FEL as the active gain medium are given in Section 4.

2. BARE CAVITY SIMULATIONS

Prior to this work, FELEX was primarily used to investigate the operation of FELs employing stable resonators. One primary difference between stable and unstable resonator simulations is the high transverse spatial frequencies introduced by aperturing (or scraping) in the unstable direction. Owing to the discrete nature of the simulation, the discontinuity in the optical field imposed by these apertures can give rise to aliasing of the field at subsequent propagation locations. The following three techniques were used to control these high spatial frequency components.

- **Aperture Apodisation:** the transmission (T) of the optical field near the edge of hard apertures was

changed from a step function to a smoothly varying sinusoidal function of the form

$$T = \frac{1}{2} \left\{ 1 + \sin \left[\frac{\pi}{2} \frac{x - x_{ap}}{h_{ap}} \right] \right\} \quad |x - x_{ap}| \leq h_{ap} \quad (1)$$

- where x_{ap} is the location of the aperture edge and h_{ap} is the half-width of the apodisation region. The half-width is specified by an integer number of grid points and was typically 2 to 4 depending on the grid resolution. Although the field values on the grid are a piecewise approximation of the expression in Eq.(1), significant reductions in aliasing can be achieved with apodisation over just a few grid points. Care was taken to keep the half-width of the apodisation region small enough so that the physics of the problem being studied was not altered. The cavity mode would be significantly changed if the deviation in the radius of the aperture introduced by the apodisation modified the equivalent Fresnel number of the resonator by unity. Therefore, the half-width of the apodisation was chosen to keep $\Delta N_{eq} \ll 1$.
- Spatial Frequency Filtering: The algorithm used to propagate the optical field in free-space involves the use of fast Fourier transforms (FFT). In transform space the large wavenumber values will appear at the edges of the 2-D field array. These large wavenumber field components can be suppressed by applying an apodised "wavenumber aperture" to the electric field transform array. In FELEX this filter has the form

$$T_k = \frac{1}{2} \left\{ 1 - \cos \left[\pi \frac{k/k_{max} - k_{ap}/k_{max}}{1 - k_{ap}/k_{max}} \right] \right\} \quad (2)$$

where k_{max} is the maximum wavenumber allowed by the grid such that k_{ap}/k_{max} is the normalised input wavenumber specifying where the filtering begins. As with the spatial apodiser, one must take care not to change the problem by excessively filtering in Fourier space. A reasonable guideline for the truncation of spatial frequencies is given by

$$\lambda_{min} \leq \frac{\text{Fresnel zone}}{5} \quad (3)$$

where λ_{min} is the shortest transverse wavelength remaining after filtering. When employed, this filtering procedure is performed at each propagation step through the resonator.

- Aperturing at a Focus: Since the optical field profile at a focus is just a scaled version of the Fourier transform of the electric field, one can filter out the high frequency spatial components by introducing an aperture at the focus that scrapes off the wings of the field. The application of this technique differs from the above case in that the truncation of the higher spatial frequencies is imposed more abruptly and at only specific positions in the resonator.

Cavities with low equivalent Fresnel numbers were modeled using one or more of the previously described filtering techniques to control aliasing. Low Fresnel number cavities were chosen to minimise the amount of transverse resolution required to adequately resolve the problem. A transverse grid of 128×128 was commonly used. The propagation algorithm used an expanding grid coordinate system, similar to that described by Sasiela and Siegman⁸. The size of the grid was initially set equal to 2.5 times the geometric size of the beam in the resonator. When modeling resonators with symmetric scrapers, an interpolator was used to magnify the remaining field, thereby maintaining optimum resolution.

As an initial test case, a symmetric standing-wave resonator with $M = 1.42$ and $N_{eq} = .52$ was chosen. The mode profile obtained was in close agreement with that given by Renach and Chester⁹.

Next, an attempt to model a confocal ring resonator with $M = -1.42$, and $N_{eq} = -3.12$ was made. The ring configuration is shown in Figure 2. Note that the ring incorporates transmissive optics while an actual high-power resonator would employ cylindrical or spherical mirrors. Although the ring has a negative magnification and equivalent Fresnel number (owing to the intracavity focus), the mode pattern at the output scraper will be identical to the mode pattern on either mirror of a positive branch symmetric resonator if the magnitudes of M and N_{eq} for the two resonators are identical. To calculate the Fresnel number of the ring we use the property² that the reciprocal of the cavity Fresnel number is equal to the sum of the reciprocal

Fresnel numbers of the individual segments of the cavity. With the help of Figure 2, the collimated Fresnel number of the ring can be expressed

$$N_c^{-1} = \frac{\lambda}{a^2} \left[L_1 - \frac{L_2}{M} + \frac{L_3}{M^2} \right] \quad (4)$$

where a is the aperture half-width. Using this relation in conjunction with the expression for N_{eq} given by

$$N_{eq} = \frac{M^2 - 1}{2M^2} N_c \quad (4)$$

the various cavity lengths can be chosen to obtain the desired M and N_{eq} .

Initial simulations produced mode patterns that deviated significantly from those given by Rensch and Chester⁶. However, by placing an aperture at the intracavity focus, an intensity profile closely resembling the pattern given in [6] was achieved. Figure 3a and 3b show the mode pattern from [6] and from the PELEX simulation with focal aperturing. Since the exact filtering algorithm used in [6] was not specified by the authors, a closer comparison could not be performed. An additional comparison was made of the mode pattern obtained analytically by Rodgers and Ertkila⁷. They conducted calculations for a standing-wave resonator with $M = 2.5$ and $N_{eq} = 3.12$. This resonator was modeled again using a negative branch ring configuration with the same parameter magnitudes. To control aliasing, apodisation over 4 grid points was employed and an aperture was placed at the focus. The lowest order mode pattern from their paper is given in Figure 4a while the simulation result is given in Figure 4b. The results of these comparisons indicated that the FFT propagator in PELEX was adequate for modeling unstable resonator geometries.

3. EXPERIMENTAL COMPARISON

A stable-unstable ring laser has been constructed at MRC-Albuquerque. The resonator has near confocal geometry with astigmatism introduced to make the ring unstable in one dimension. The magnification of the cavity was kept low ($|M| \approx 1.2$) to limit the the output coupling. This keeps the saturated single-pass gain of the FEL relatively low ($10 \approx 30\%$). As a result, the amount of mode distortion⁸ caused by the gain in the narrow electron beam will not significantly alter the mode shape of the bare-cavity resonator. In the experiment a laser dye tube provided the active gain media.

The equivalent resonator depicted in Figure 5 was used to model the experimental resonator. The simulation converged after approximately 20 passes to a loss of $\approx 14\%$ per pass. Transverse profiles in the unstable direction of the experimental mode and the mode from the simulation are shown in Figure 6. Clean gaussian mode profiles were obtain in the orthogonal transverse plane both experimentally and in the simulation.

4. STABLE-UNSTABLE FEL SIMULATIONS

A modification of the propagation algorithm had to be made before the FEL interaction could be included in the simulation model. PELEX uses a fixed (non-expanding) grid inside the wiggler. A finite difference algorithm is used in this region so that the optical source due to the electrons can be added in as the optical field is stepped through the wiggler. As a final check, the finite difference propagator was tried through the wiggler region with no electron beam present. The results obtained were identical to the previous simulations using only the FFT propagator.

A scaled (with identical M and N_{eq}) version of the experimental stable-unstable ring analysed in Section 3 was modeled. The cavity dimensions were increased so that the Rayleigh range was equal to the length of typical experimental wigglers (≈ 1 meter). Approximately 20 passes were required for the optical mode to converge in the unstable direction. Then, depending on the amplitude of the initial optical field, the circulating power in the cavity increased until saturation was reached. A 3-D plot of the transverse electric field at the end of the wiggler is given in Figure 7. The mode in the unstable direction has several side lobes (caused by the high transverse spatial frequencies) while the mode in the stable direction has a narrow gaussian dependence. The size of the optical mode was chosen so that the central lobe of the optical mode

was approximately twice the size of the electron beam. This assured that virtually all the electrons interacted efficiently.

The output beam scraped off one side of the unstable direction in the back leg of the resonator is shown in Figure 8a. Since the beam is unobscured, it can be focused to a narrow spot as shown in Figure 8b. This focusing ability is crucial for applications where high intensity is desired.

5. CONCLUSIONS

We have shown that FELEX is an effective tool for addressing the usefulness of stable-unstable resonators for free electron laser applications. Good agreement has been obtained both with previously published unstable mode profiles and with the experimentally measured mode profiles of the stable-unstable laser currently operating at Mission Research Corporation in Albuquerque. The simulations show that a clean output beam can be obtain using an asymmetric scraper in conjunction with the stable-unstable FEL cavity configuration. More simulations will be required to determine the operating characteristics of such resonators for high power applications.

6. ACKNOWLEDGMENTS

The authors would like to thank Dr. B. D. McVey of Los Alamos National Laboratory for his helpful suggestions concerning the operation of FELEX. This work supported by the Strategic Defense Initiative Organization.

7. REFERENCES

1. R. L. Tokar, B. D. McVey and J. C. Goldstein, "Sideband Suppression in Free Electron Lasers using a Grating Rhomb", *IEEE J. Quantum Electronics*, June, (1988).
2. A. H. Paxton, "Unstable resonators with Negative Equivalent Fresnel Numbers", *Optics Letters*, 11, 76-78, (1985).
3. R. W. Jones, C. Casen and J. F. Perkins, "New Laser Resonator with Unobscured Reflective Outcoupling and Internal Optic Axis", Paper presented at the AIAA 19th Fluid Dynamics, Plasma Dynamics, and Laser Conference, held in Honolulu, Hawaii, June 8-10, (1987).
4. B. D. McVey, "Three-Dimensional Simulations of Free Electron Laser Physics", *Nucl. Instrum. Methods in Phys. Res.*, A250, 449-455, (1986).
5. E. A. Sasikas and A. E. Siegman, "Mode Calculations in Unstable Resonators with Flowing Saturable Gain. II: Fast Fourier Transform Method", *Applied Optics*, 14(8), 1874-1889, (1975).
6. D. B. Rensch and A. N. Chester, "Iterative Diffraction Calculations of Transverse Mode Distributions in Confocal Unstable Laser Resonators", *Applied Optics*, 12(5), 997-1010, (1973).
7. M. E. Rodgers and J. H. Erkkila, "Resonator mode analysis using linear Prolate Functions", *Applied Optics*, 22(13), 1992-1995, (1983).
8. B. D. McVey with R. W. Warren, "Bending and Focusing Effects in a FEL Oscillator (I: Numerical Simulations", *Nucl. Instrum. Methods in Phys. Res.*, A259, 158-162, (1987).

DISCLAIMER

This report was prepared as an account of work sponsored by an agency of the United States Government. Neither the United States Government nor any agency thereof, nor any of their employees, makes any warranty, express or implied, or assumes any legal liability or responsibility for the accuracy, completeness, or usefulness of any information, apparatus, product, or process disclosed, or represents that its use would not infringe privately owned rights. Reference herein to any specific commercial product, process, or service by trade name, trademark, manufacturer, or otherwise does not necessarily constitute, or imply its endorsement, recommendation, or favoring by the United States Government or any agency thereof. The views and opinions of authors expressed herein do not necessarily state or reflect those of the United States Government or any agency thereof.

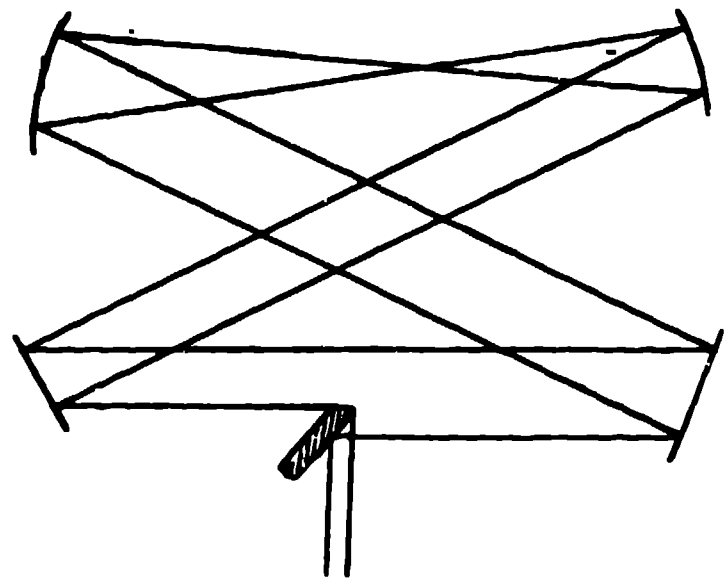


Figure 1. Stable-unstable ring with asymmetric edge scraper.

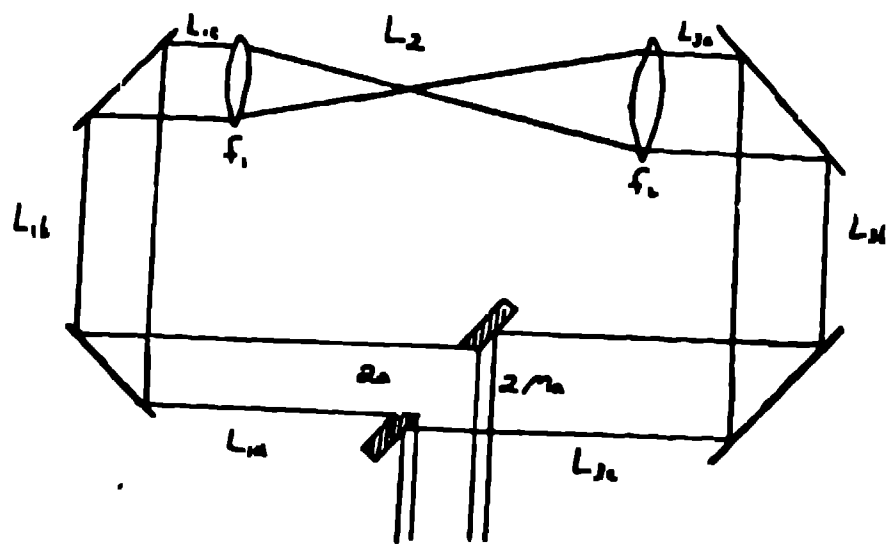


Figure 2. Unstable ring resonator with symmetric halo scraper.

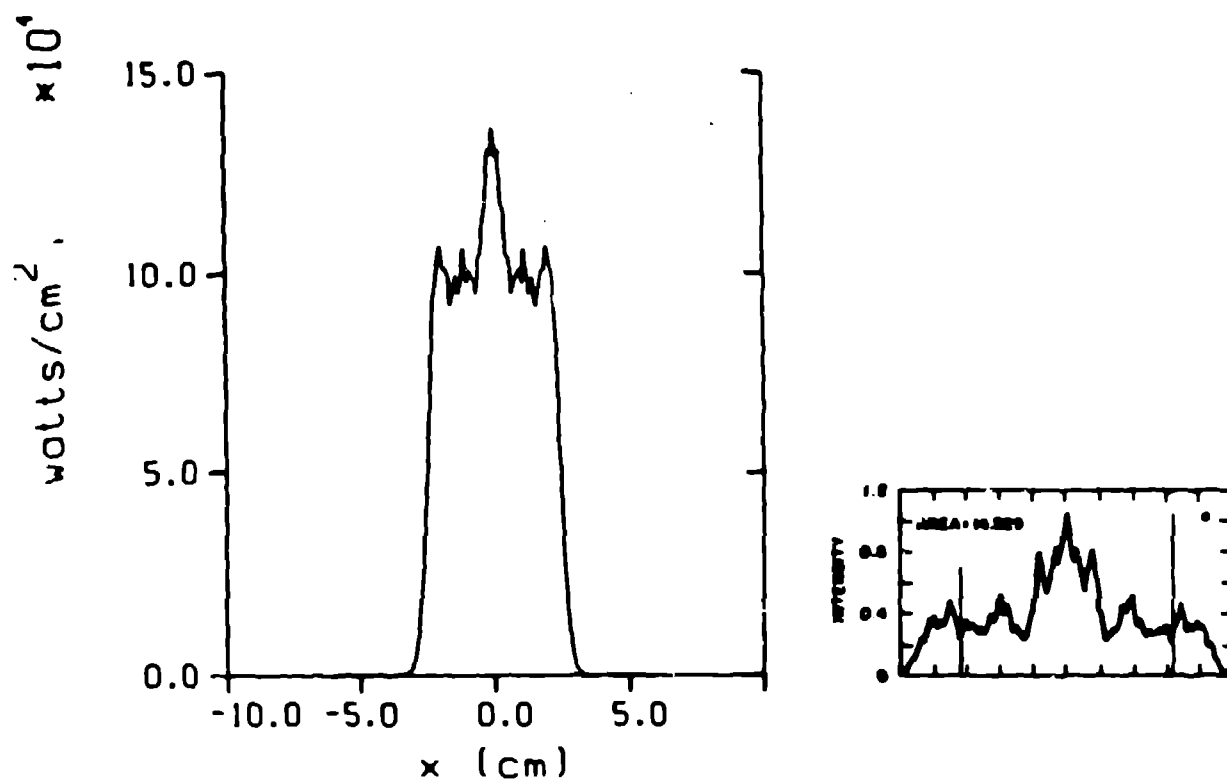


Figure 3. (a) Mode profile for $M = 1.42$, $N_{av} = 3.12$ anstable resonator from Renach and Chester⁶; and (b) Simulation of a negative branch unstable ring resonator with the same magnitude parameters.

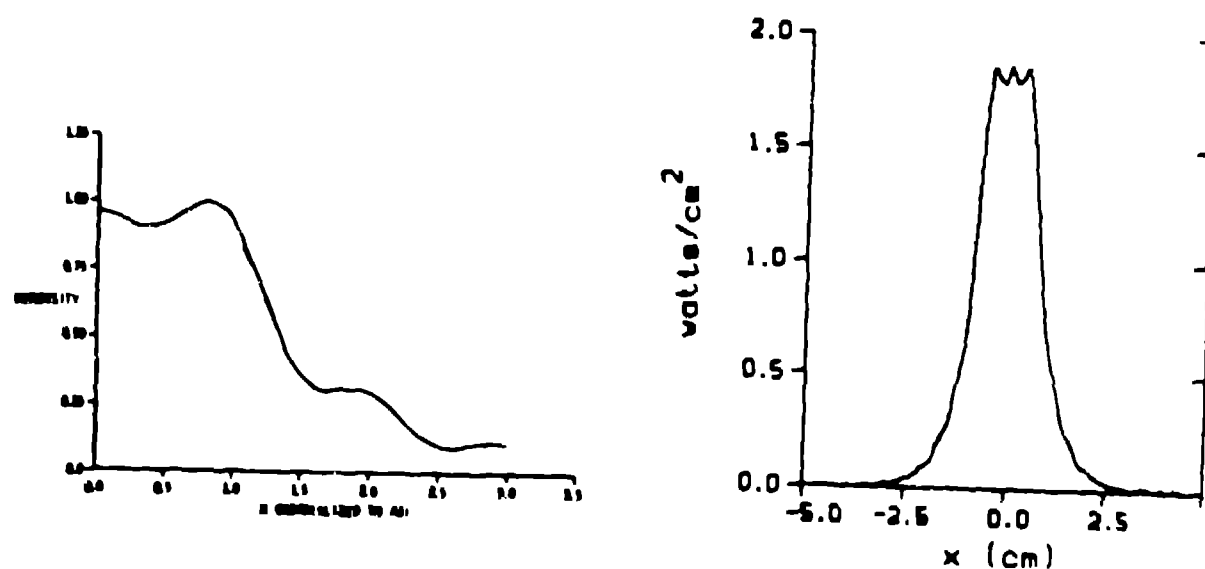


Figure 4. (a) Analytically obtained mode profile of a $M = 2.5$, $N_{av} = 3.12$ anstable resonator from Rodgers and Ekkila⁷; and (b) Simulation of a negative branch unstable ring resonator with the same magnitude parameters.

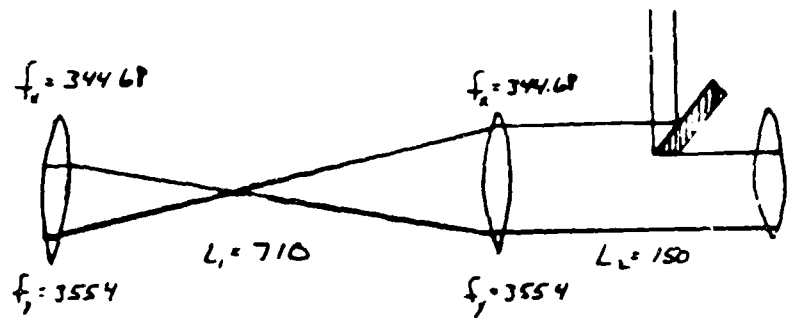


Figure 5. Equivalent stable-unstable model of the experimental resonator with asymmetric scraper.

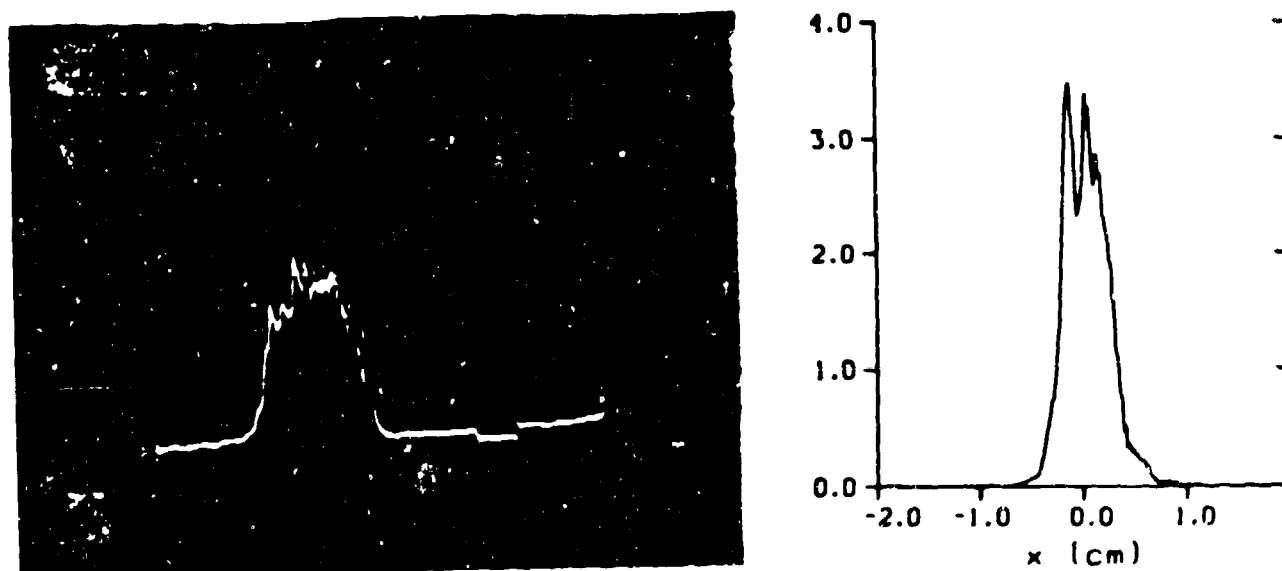


Figure 6. (a) Experimental mode profile in the unstable direction taken at one of the mirrors; and (b) mode profile at the same position from the simulation.

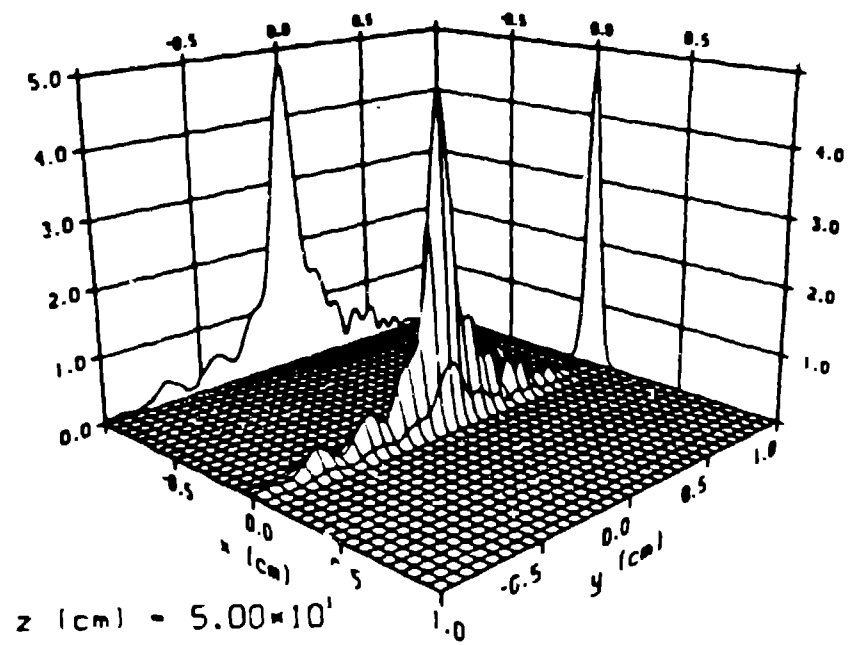


Figure 7. Three-dimensional transverse electric field profile of the stable-unstable FEL oscillator near the intracavity focus.

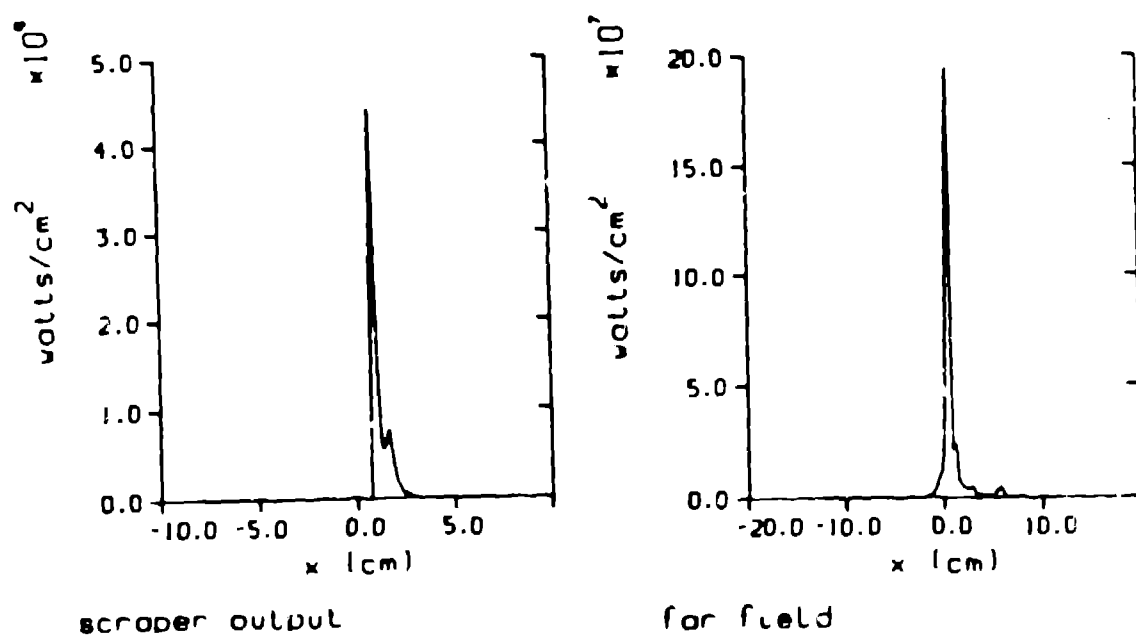


Figure 8. (a) Output beam of the stable-unstable FEL oscillator; and (b) far field pattern of the output beam in (a).